



Diatom dynamics during the last six centuries in Lake Odensjön: a new varved sediment record from southern Sweden

Ethan L. Silvester · Karl Ljung · Richard Bindler · Hanna Hertzman ·
Giulia Lodi · Dan Hammarlund

Received: 23 March 2024 / Accepted: 8 August 2024
© The Author(s) 2024

Abstract Varved lake sediments offer valuable insight into past environmental conditions with high temporal resolution and precise chronological control. A combination of diatom and geochemical analyses of the recently deposited sediments of Odensjön, a small dimictic lake in southern Sweden, shows alternating light and dark laminae composed of greater amounts of biogenic silica and organic matter, respectively. As confirmed by independent radiometric dating and Pb pollution data, and supported by scanning electron microscopy of individual laminae, these features represent ongoing deposition of biogenic varves. Corresponding diatom and geochemical data obtained from a 92-cm long freeze core provide evidence of substantial lake-ecosystem dynamics during the last six centuries, related mainly to variations in light penetration

and wind shear driven by human-induced changes in catchment vegetation. The diatom assemblage of Odensjön's varved sediments is dominated by planktonic species, primarily *Asterionella formosa*, *Fragilaria saxoplanktonica* and *Discostella lacuskarluki* during periods of forest cover, while increased catchment openness from the mid-1500s to the late 1800s led to increased abundance of *Lindavia comensis*. Long-term variations in climate and land use, mediated through changing length of the ice-cover season and nutrient input, respectively, probably contributed to the observed trends, as well as to variations in the appearance and visibility of the varve record across the sampled sediment sequence. Odensjön represents the southernmost varved sediment record in Fennoscandia documented to date, offering potential to study the effects of various types of external forcing on its sensitive lacustrine ecosystem since the Late Weichselian deglaciation. In the present study, we investigated the possibility of assessing the local impacts of two major, historically documented volcanic events, Laki 1783–84 and Tambora 1815, which are known to have affected European societies. Although the mildly alkaline waters of the lake are well buffered and hence relatively resilient to volcanic acid deposition, a minor response to the Laki eruption may be recorded in the diatom stratigraphy.

Supplementary Information The online version contains supplementary material available at <https://doi.org/10.1007/s10933-024-00338-8>.

E. L. Silvester (✉) · K. Ljung · H. Hertzman · G. Lodi ·
D. Hammarlund
Department of Geology, Lund University, 223 62 Lund,
Sweden
e-mail: ethan.silvester@geol.lu.se

R. Bindler
Department of Ecology and Environmental Science, Umeå
University, 901 87 Umeå, Sweden

G. Lodi
Department of Biology, University of Antwerp, Antwerp,
Belgium

Keywords Limnology · Climate · Stratification ·
Cyclotella · Land use · Acidification

Introduction

Lakes support diverse ecosystems and play an important role in the terrestrial biosphere. Under certain conditions lake sediments present varves, which are an annual succession of layers, or laminae, composed of material deposited during different seasons of the year (Zolitschka et al. 2015). Varved sediment records have frequently been used to investigate changes in environmental conditions over time and provide insights into past land-use dynamics (Rey et al. 2017; Dubois et al. 2018) and climate variability (Linderholm et al. 2018). Such records also offer advantages for studying abrupt events of local, regional and worldwide significance, such as volcanic eruptions, potentially revealing both direct and lagged biogeochemical responses of lake ecosystems and their catchments (Bonk et al. 2023). Varved lake sediments are widely documented across central and northern Fennoscandia (Ojala et al. 2000; Zillén 2003; Zolitschka et al. 2015), although few such records have been documented in its southern regions.

The eruptions of Laki in Iceland (1783–84 CE) and Tambora in Indonesia (1815 CE) are two of the most well-documented volcanic events in recent centuries, with far-reaching impacts on the environment and society. The eruption of Laki was associated with famine and crop failures in northern and central Europe, resulting from sulphur deposition (Grattan and Charman 1994). The eruption of Tambora resulted in worldwide cooling with impacts lasting multiple subsequent years (Oppenheimer 2003; Brönnimann and Krämer 2016). While the environmental impacts of Tambora 1815 generally led to changing hydroclimate (Brönnimann and Krämer 2016), sulphur deposition from Laki 1783–84 is likely to have reached southern Sweden as indicated by reconstructed sulphate aerosol concentrations (Balkanski et al. 2018). Lake sediments deposited during recent centuries commonly reside within the uppermost parts of paleoenvironmental records, and the potential impacts of these eruptions are therefore often difficult to separate from other concurrent environmental stressors, including anthropogenic impacts.

Diatoms form a major component of the algal communities in freshwater ecosystems and are known to respond rapidly to environmental change (Dixit et al. 1992). Diatoms preserved in lake sediments are therefore widely used in paleoecology, for example

for reconstruction of lake-water pH and surface temperature (Cameron et al. 1999; Rosén et al. 2000), and highly resolved diatom records have previously revealed the impacts of volcanic acid deposition (Payne and Egan 2019).

This study first aims to document the character and formation processes of the previously undescribed, potentially varved sediment record of Lake Odensjön in southernmost Sweden. Second, using diatom and geochemical analyses, we aim to assess the ecological and biogeochemical responses of the lake and its catchment to natural and anthropogenic environmental changes during recent centuries. Third, we also aim to evaluate the potential of this unique sediment record for studies of transient, externally forced environmental perturbations, by attempting to identify signals of Laki (1783–84 CE) and Tambora (1815 CE) using a sub-decadal sampling resolution.

Site description

Odensjön (56° 0′ 13.9″ N, 13° 16′ 32.2″ E) is a small lake situated in the Söderåsen National Park in southernmost Sweden (Fig. 1). The lake occupies a presumably pre-Weichselian glacial cirque incised into the Söderåsen horst ridge (Rapp 1984). The steep sides of the basin, which may have been accentuated by nivation processes during the Late Weichselian, are covered by scree dominated by angular stones and boulders. The lake is approximately 140 m in diameter and situated in a small catchment with a northward-flowing outlet joining the Nackarpsdalen Valley (Fig. 1). The backwall of the basin extends about 35 m higher than the lake surface at 62 m a.s.l. The lake is predominantly groundwater-fed, dimictic and has a maximum depth of 21.4 m (Godlund 1951). The outlet flows initially through peat atop till. Its approximately 5.5-m thick sediment sequence extends to the Late Weichselian, primarily consisting of clay gyttja (Berglund and Rapp 1988). Water sampling in the national monitoring program (Riksinventeringar av sjöar och vattendrag) in late autumn of 2012 and 2018 yielded pH values of 7.17 and 7.27, and conductivities of 14.92 and 14.60 mS m⁻¹, respectively (SLU 2024). The catchment of the lake is located on crystalline bedrock consisting of granitic gneiss with abundant outcrops. The immediate surroundings are composed of sandy till with a clay content of 5–15%, and a nearby glaciofluvial deposit is devoid

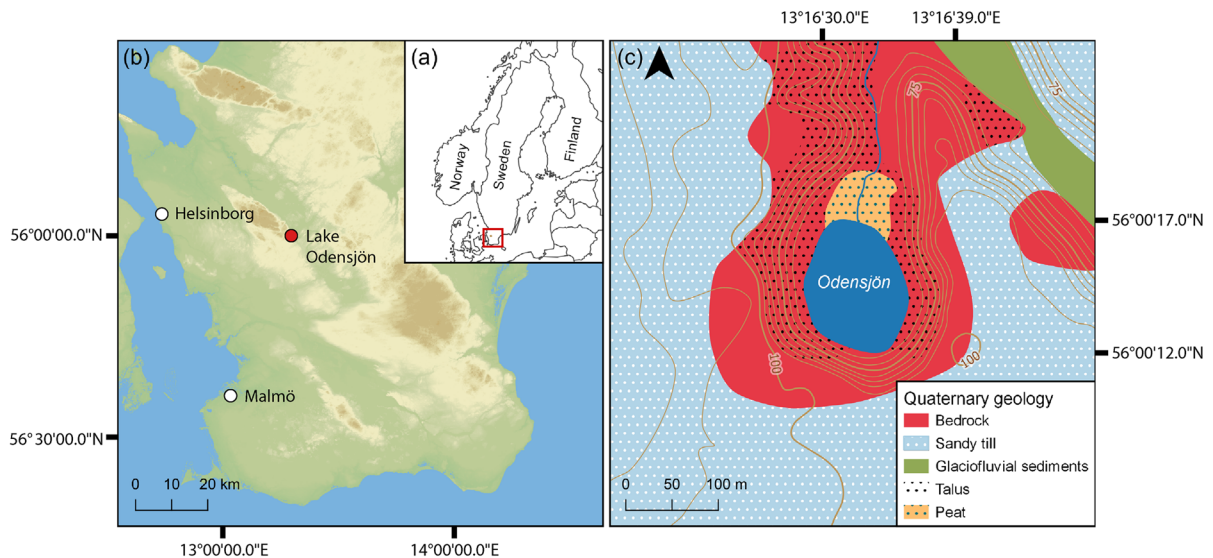


Fig. 1 **a** Location of Lake Odensjön in southernmost Sweden. **b** its relation to major topographic features in the region. **c** the distribution of Quaternary deposits in the catchment and adjacent areas. Contour lines in **c** are given at 5-m intervals

of carbonates (Ringberg 1984). A narrow curtain of alder, birch and other deciduous trees occurs at the lake margin while the talus slopes of the catchment are covered partly by beech trees.

Mean annual precipitation is 839 mm (of which 58% falls during July–December) and about 500 mm is lost by evapotranspiration. Mean annual air temperature is 8.2 °C, and mean January and July air temperatures are 0.2 °C and 17.3 °C, respectively. These data, representing reference normals for the period of 1991–2020, were compiled by the Swedish Meteorological and Hydrological Institute based on monitoring data from Ljungbyhed (43 m a.s.l.), 8 km north-west of the study site.

Materials and methods

Core treatment and sampling

A sediment freeze core was obtained from the central part of the lake at 19.9 m depth in February 2017 using the sampling device described by Renberg and Hansson (2010). The core was transported frozen to storage in a freezer room and yielded two matching adjacent slabs after cleaning and cutting, Od17A and Od17B hereafter, each containing approximately 92 cm of sediments.

From Od17A, samples at 2-cm contiguous intervals were obtained for dating as part of a M.Sc. project (Hertzman 2021). From Od17B, using two thirds of its width, a total of 46 sediment samples were obtained under frozen conditions at 2-cm intervals covering 92 cm for diatom and geochemical analyses. To assess diatom-assemblage dynamics at greater temporal resolution at 32–56 cm depth, an additional 24 samples were obtained at 1-cm intervals from the remainder of Od17B. Samples were freeze-dried and homogenised before collection of aliquots for various analyses.

To assess seasonal differences in the diatom assemblage, seven individual laminae from the uppermost part of the sediment record from Od17B (Fig. 3) were sampled using a scalpel under frozen conditions. The structure of multiple laminae from a sample at 18–20 cm depth remained undisturbed after freeze-drying and was subject to additional geochemical analyses to identify relative differences in composition.

Chronology

A total of 17 freeze-dried samples from the top 33 cm were submitted to the Environmental Radiometric Facility, University College London, to obtain ^{210}Pb , ^{226}Ra , ^{137}Cs and ^{241}Am activities by direct gamma

assay using an ORTEC HPGe GWL series well-type coaxial low background intrinsic germanium detector. Sediment ages were determined using the Constant Rate of Supply (CRS) ^{210}Pb model (Appleby 2001) and confirmed by ^{137}Cs and ^{241}Am data. Additionally, three radiocarbon dates were obtained using macroscopic plant remains collected at the depths of 68.7, 76.0 and 88.5 cm (Table S1). An age model for the sediment sequence was established based on the combination of ^{210}Pb and ^{14}C dates, using a polynomial fit with a smoothing of 0.6 in the R package CLAM (Blaauw et al. 2021). All dates given refer to the common era (CE).

Sediments from Od17A were imaged after a short exposure to room temperature to allow surface oxidation, improving the visual contrast between laminae. Couplets of light and dark laminae, potentially representing varves, were counted using the program ImageJ (Collins 2007). Counting of lamina couplets was performed to a depth of 82.5 cm. In some sections of the record the couplets appeared discontinuous or poorly visible, which prevented counting. To account for this, we produced a corrected lamina couplet count, applying adjustments using a linear interpolation of the average thickness of lamina couplets above and below each uncountable section, covering a distance equal to the width of the uncountable section.

Geochemical analyses

Scanning electron microscopy (SEM) and energy-dispersive X-ray spectroscopy (EDS) were used to assess the elemental composition of intact laminations at 18–20 cm depth. Qualitative analysis was performed using a Tescan Mira3 high-resolution Schottky FE-SEM equipped with an Oxford EDS detector at the Department of Geology, Lund University. Samples were imaged at 2 kV and elemental mapping was performed at 15 kV. EDS was performed to map elements detected by surface scans. Multiple scans were performed to confirm consistent transitions in the major elemental components between neighbouring laminae.

Semi-quantitative XRF measurements were performed to identify stratigraphic changes in elemental composition. A Bruker S1 Titan handheld XRF at the Department of Ecology and Environmental Science, Umeå University, was used to obtain measurements

of ~200 mg freeze-dried aliquots. Trace elements and elements with low values and large uncertainties based on regular duplicates were excluded. The elements Al, Ca, Fe, K and Mn and S are shown constrained by the predominantly allochthonous element Ti. Because potassium [K] is susceptible to leaching from silicate minerals, we use the K/Ti ratio as a proxy for weathering (Arnaud et al. 2012). Additionally, we present and assess the use of the Mn/Fe ratio as an indicator of oxygenation (Melles et al. 2012) and the Ca/Fe ratio as an indicator of pedogenic input (Elbert et al. 2013).

Total organic carbon (TOC) and total nitrogen (TN) contents were determined by elemental analysis using a Costech ECS4010. Approximately 5 mg of freeze-dried material from each sample was loaded into Ag capsules. The samples were decalcified using acid fumigation with concentrated HCl in a desiccator (Komada et al. 2008). The decalcified samples were wrapped in Sn capsules before analyses. Elemental C/N ratios were converted to atomic ratios by multiplication with 1.167.

The content of biogenic silica (BSi) was measured following DeMaster (1981) and Conley and Schelske (2001). A weak base of 1% Na_2CO_3 was used for digestion at 85 °C in a shaking water bath and extractions were taken after 3 h, 4 h and 5 h, and neutralised with HCl before cooling, using frequent duplicates. To quantify the dissolved silicon (dSi) content, ammonium molybdate was added for spectrophotometric measurement of molybdate-blue using a Smartchem 200 (AMS System) wet chemical analyser. BSi concentrations were determined by the intercept of a least-squares regression of extracted dSi data.

Diatom analysis

Microscope slides for diatom analysis were produced using 0.10–0.15 mg aliquots from each sample. Using the water bath method (Renberg 1990), samples were treated with 37% HCl to dissolve trace amounts of calcium carbonate and 33% H_2O_2 to remove organic material. Treated samples were mounted to clean glass coverslips using Naphrax resin (refractive index 1.73). For all samples, a minimum diatom counting efficiency (DCE) of 92.9% was achieved (Pappas and Stoermer 1996). At least 400 valves were counted for 2-cm

samples (DCE \geq 92.9%) and individual laminae (DCE \geq 94.0%). At least 350 valves were counted for 1-cm samples (DCE \geq 93.2%). Diatom identification employed modern resources (Lange-Bertalot et al. 2017) and updated nomenclature including Nakov et al. (2015). Small diatom species were inspected via SEM. Specifically, this confirmed the presence of *Discostella lacus-karluki* (Manguin ex Kociolek & Reviere) Potapova, Aycock & Bogan, which is easily confused with similar species (Potapova et al. 2020). Siliceous stomatocysts produced during the resting stage of chrysophytes were counted in addition to diatoms to provide complementary information on ecosystem conditions (Smol 1985).

The species *Fragilaria tenera* Smith, *Fragilaria tenera* var. *nanana* Lange-Bertalot and *Fragilaria saxoplanktonica* Lange-Bertalot & Ulrich were identified using Lange-Bertalot et al. (2017). *Fragilaria tenera* was differentiated from *F. saxoplanktonica* and *F. tenera* var. *nanana* by clearer striae and a wider, shorter valve. Furthermore, *F. tenera* var. *nanana* was more strongly associated with *F. saxoplanktonica* than with *F. tenera*, and *F. tenera* was by far the least abundant of the three throughout our record. Difficulties in the identification of, and between, *F. saxoplanktonica*, *F. tenera* var. *nanana* and *F. tenera* have been outlined by Kahlert et al. (2019) and Williams (2019). We consider *F. tenera* var. *nanana* and *F. saxoplanktonica* collectively here as *F. saxoplanktonica*, because the predominant difference observed in our samples was a longer valve length and curvature in specimens recorded as *F. saxoplanktonica*, which is a weak criterion for differentiation.

A stratigraphically constrained incremental sum of squares clustering (CONISS) was performed (Fig. S1) to determine diatom-community zones (D1-5). Shannon's Index (H) was used as a measure of alpha diversity of the diatom assemblage. The proportion of planktonic relative to benthic diatoms was used as an indication of functional differences over time based on growth habits, given as percentages of planktonic (and tychoplanktonic) diatoms. Because bloom timing and physicochemical optima differ between planktonic species, we also calculated the proportion of centric to pennate species within the planktonic fraction of the assemblage, presented as a percentage of centric diatoms relative to the planktonic fraction. The ratio of diatom frustules to

chrysophyte stomatocysts in each sample is given as the percentage of diatom frustules relative to the sum of diatom frustules and chrysophyte stomatocysts.

Statistical analysis and diatom-inferred pH reconstruction

To characterise potential relationships between different geochemical data, a principal component analysis (PCA) was performed with Canoco 5 (Šmilauer and Lepš 2014) using XRF, BSi, TOC and TN data. Samples were not included in the PCA when measurements for any single category of data were not available, which was the case for the uppermost sample (0–2 cm depth), samples at 44–46 cm and 66–68 cm, and the lowermost six samples (80–92 cm). The PCA was performed on square-root transformed data from 37 samples at 2–80 cm depth.

A diatom-inferred pH reconstruction (DI-pH) was produced using weighted-averaging partial least squares (WA-PLS) with training-set data from the Surface Water Acidification Project (SWAP; Battarbee and Renberg 1990). Taxa were assigned 'EDDI' codes following the European Diatom Database Initiative (EDDI, Battarbee et al. 2001) for harmonisation with the SWAP training data. The diatom taxa included in the pH reconstruction composed an average proportion of $55.7 \pm 19.27\%$ (σ) of assemblages across all samples.

Results

Lithostratigraphy

The sediments were divided into seven lithostratigraphic units (Fig. 2). Table 1 provides an overview of the differences between each unit and their corresponding ages according to our age model (Fig. 2). Unit I consists of pale brown fine-detritus gyttja, in which thick, light laminae are sporadically present. Sediments in unit II are rusty brown and contain the thinnest laminae couplets recorded (1.0 ± 0.3 mm), where laminae have a patchy microstructure but remain visible. Unit III is the thickest unit (26.4 cm), where couplets remain thin, and light laminae are poorly discernible in some sections. Fragmented leaves, which are occasionally present in units I and II are largely absent from units III–V where couplets

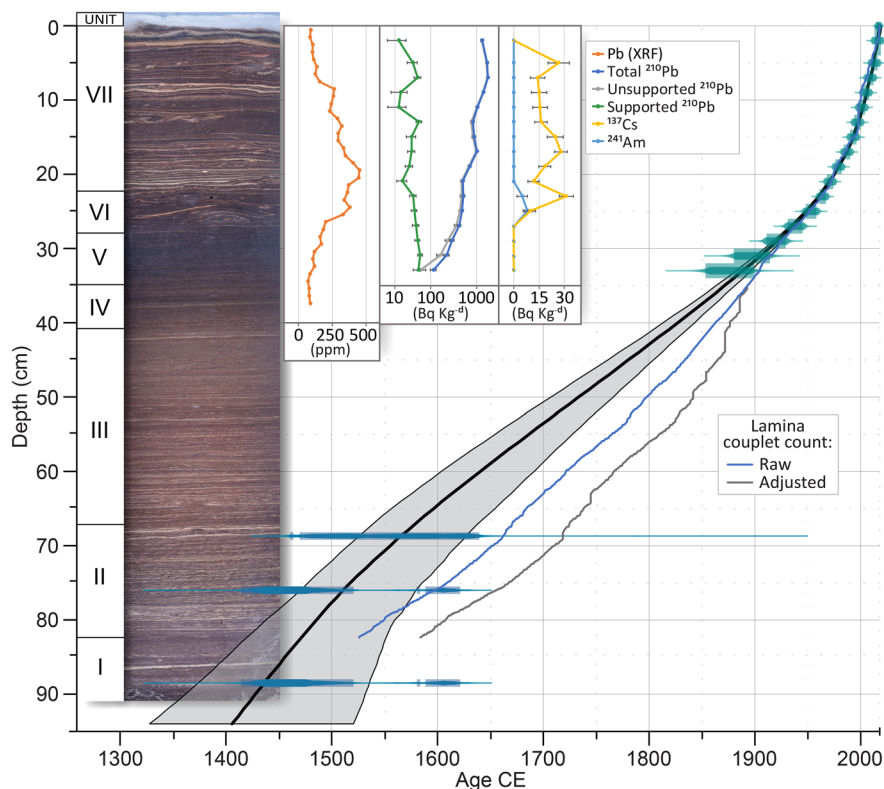


Fig. 2 Age-depth model (black line with uncertainty envelope at double standard deviation level in grey) for the studied sediment sequence from Odensjön based on ^{210}Pb (green bars with uncertainty envelopes) and ^{14}C dates (blue bars and lines representing 68% and 95% probability envelopes, respectively). Lithostratigraphic units I–VII are shown next to a photograph of the sediments. Inset graphs show ^{210}Pb , ^{137}Cs and ^{241}Am

gradually increase in thickness to 1.7 ± 0.6 mm in unit V. From unit IV both light and dark laminae become darker, with the poorest contrast in unit V. Unit VI is characterised by the appearance of deciduous leaves, which occasionally intersect multiple laminae in units VI and VII, resulting in a partial displacement of some laminae but no significant mixing of material. Unit VII represents the poorly compacted top sediments, which return to a lighter colour and contain clearly distinguishable lamina couplets.

Sediment composition and diatom seasonality

The poorly compacted top sediments are characterised by 2–5 mm thick individual laminae (Fig. 2). Based on SEM observations, the light laminae are composed predominantly of diatoms, while the

data used for constraining the ^{210}Pb CRS model in addition to XRF-based Pb data for the uppermost 37 cm, yielding independent support to the radiometrically based age model. Grey and blue lines represent ages based on cumulative counts of lamina couplets, where the grey line is the raw count and the blue line represents the adjusted lamina record

intervening dark laminae consist of a matrix dominated by detritus, and also proportionally smaller amounts of diatoms (Fig. 3). The light laminae appear to contain an abundance of planktonic species including *Asterionella formosa* Hassal and different *Fragilaria*, with little contribution from centric species. Benthic species are scarce but more abundant in the dark laminae, which are dominated by centric species of *Lindavia* and *Discostella*. Both *Lindavia radiosa* Grunow and *Lindavia comensis* Grunow in Van Heurck are consistently more common in the dark than in the underlying light laminae. *Discostella lacuskarluiki* comprises almost 40% of the assemblage in one dark lamina and around 25% in the underlying light lamina, whilst it is a minor component in most other laminae.

Table 1 Lithostratigraphic units and their corresponding depths and characteristic features

Lithostratigraphic unit	Depth boundary (cm)	Average sedimentation rate (mm yr ⁻¹)	Sediment characteristics		Average greyscale value	Laminae characteristics			
			Material	Leaf remains		Colouration	Average couplet thickness (mm)	Laminae colour	Continuity
						Light	Dark	Unit thickness (cm)	Unaccounted within unit (cm)
VII	0–22.5	5.8	Diatom-rich gyttja	Intact, common	Brown	Grey to light brown	Brown	22.5	4.0
VI	22.5–28	1.5			Dark brown	Brown	Dark brown	5.5	0.0
V	28–35	1.2		Fragmented, infrequent	Very dark brown	1.7 ± 0.6		7.0	0.0
IV	35–41	1.1			Dark rusty brown	1.5 ± 0.3	Light brown	6.0	2.3
III	41–67	1.1			Rusty brown	1.3 ± 0.4	Grey to light brown	26.0	6.3
II	67–82.5	1.5		Fragmented, occasional	Rusty brown	1.0 ± 0.3	Rusty brown	15.5	0.7
I	82.5–92	1.8			Pale brown	N/A: only sporadic laminae visible			

Left to right: average sedimentation rate, lithological characteristics, greyscale values (based on the averaged sediment colour in each unit) and characteristics of laminations including average couplet thickness within each unit and details of the continuity of laminations

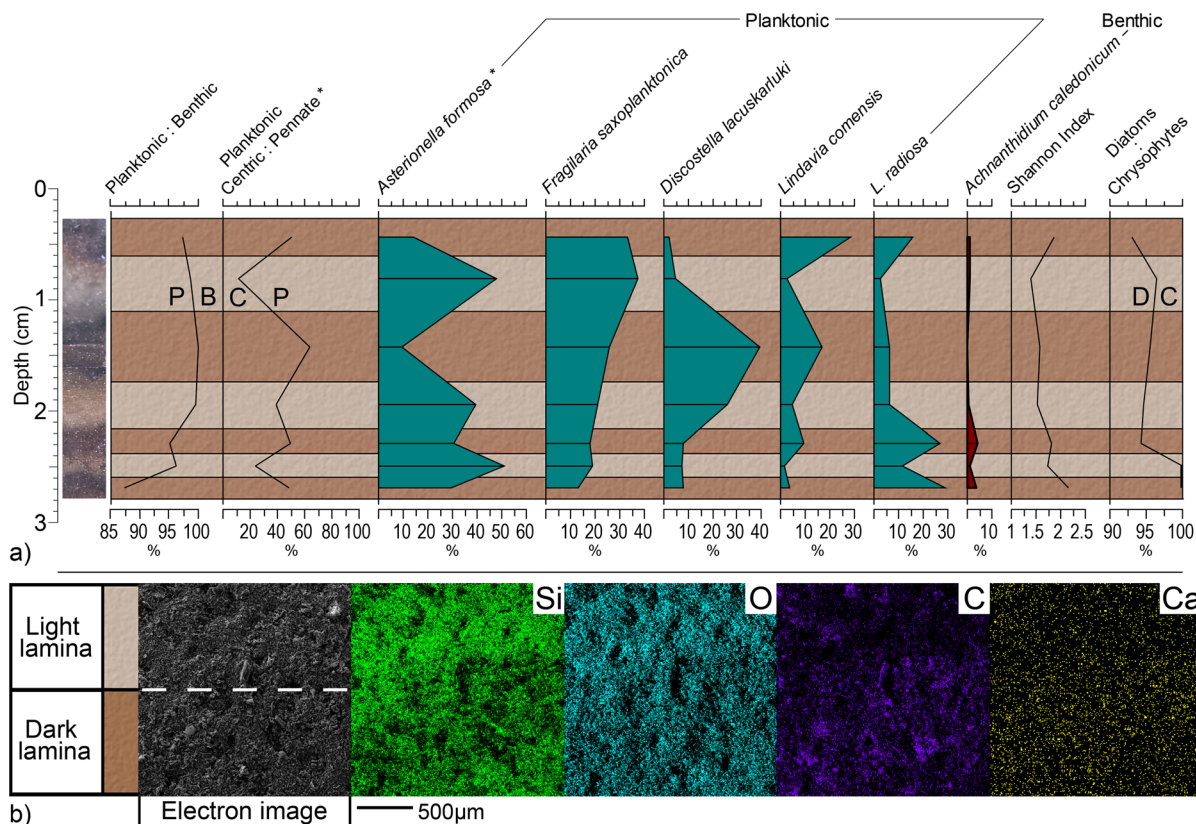


Fig. 3 **a** Dominant diatom species within each sampled lamina in the uppermost part of the sediment record (0–2.9 cm depth), shown as the relative proportions in each sample. The diatom species shown each comprise at least 3% of the assemblage in at least one of the laminae shown. An image of the sampled laminae is shown to the left. Additional parameters: the relative proportion of Planktonic to Benthic diatoms within the diatom assemblage, the relative proportions of Centric to Pennate diatoms within the planktonic fraction of the diatom assemblage, Shannon's diversity Index and the relative propor-

tions of Diatom frustules to Chrysophyte cysts. Asterisks (*) indicate parameters with statistically significant (t-test) differences between light and dark laminae. **b** SEM image of the boundary of a lamina couplet situated within a sample taken at 18–20 cm depth, showing light and dark laminae and surface EDS scans of the relative concentrations of Si, O, C and Ca in the sediments. Differences in colour intensities within each map represent the respective elemental concentrations in a semi-quantitative manner

Diatom analyses of the top seven laminae revealed six dominant species (Fig. 3a). Shannon's Index (H) ranges between 1.41 and 2.17, indicative of low diversity. Planktonic species comprise over 86% of the diatom assemblage in the inspected laminae, with minor contributions of tycho planktonic (<1.5%) and benthic (<12.6%) species. Within the planktonic fraction, centric species comprise a significantly greater proportion in the dark (48–63%) as compared to the underlying light laminae (11–38%; t-test, $p=0.02$). While H is consistently greater in the dark laminae compared to the underlying light laminae, the difference in H between light and dark laminae collectively

is insignificant (t-test, $p=0.11$). The proportion of *A. formosa* is significantly greater in light compared to dark laminae (t-test, $p=0.01$). Chrysophyte cysts were observed in five of the seven inspected laminae. The diatom-cyst ratio of lamina samples indicates that diatoms are more than 10 times as abundant as chrysophyte cysts, with little variability between laminae (Fig. 3a).

EDS measurements (Fig. 3b) show the elemental composition of the sediment surface, with colour intensities representing count rates during the mapping (scan) period. The EDS results indicate highly organic-rich sediments with a minor detrital

component. Both light and dark laminae are predominantly composed of silicon [Si] and oxygen [O], associated with diatom frustules (SiO_2), but with higher concentrations in the light laminae. The dark lamina contains a higher amount of carbon [C]. Minor amounts of calcium [Ca] are present, with slightly higher concentrations in the dark lamina.

Age model and counting of lamina couplets

The ^{210}Pb record extends to 1876 (± 12 years) at 33 cm depth (Fig. 2). In good agreement with ages inferred from the CRS ^{210}Pb model, the peaks in ^{137}Cs around 23 and 17 cm reflect maximum atmospheric fallout from atomic bomb testing in 1963 and the Chernobyl nuclear power accident in 1986, respectively. Additional independent support to these results is provided by the XRF-based Pb content record, which exhibits a distinct peak around 20 cm, most likely reflecting maximum atmospheric Pb pollution from leaded petrol in the mid-1970s (Brännvall et al. 2001). The radiocarbon dates at 76 and 88.5 cm yielded identical probability distributions. Both these dates were included in our age model, which shows increasing uncertainty ranges below 76 cm depth. The resulting age model gives evidence of variations in sediment accumulation rate, decreasing gradually from around 1.7 mm yr^{-1} in the lowermost part to an apparent minimum of around 1.0 mm yr^{-1} around 35–28 cm (unit V), then systematically increasing again to maximum values in the range of $5\text{--}10 \text{ mm yr}^{-1}$ in the uppermost, poorly compacted part of unit VII with clearly visible laminations.

Counting of lamina couplets is possible to a depth of 82.5 cm at the boundary between units I and II, below which the laminae are discontinuous. Our raw couplet count illustrates that some lamina couplets are poorly visible in unit IV and the upper part of unit V (Fig. 2). The corrected couplet count is in solid agreement with the age model to 33 cm depth (around 1900) where it is constrained by ^{210}Pb data. Below this depth there is a discrepancy between the age model and the lamina record, mostly attributed to poorly visible laminae at 36–51 cm depth, corresponding to the modelled age interval of 1859–1719. The sedimentation rate tentatively indicated by our lamina record largely agrees with that of the radiometric age model at 51–70-cm depth. Below 70 cm, the shallow gradient of the lamina record indicates a

lower sedimentation rate compared to the age model. At 77 cm depth, the corrected couplet count yields an age of 1574, which is within the upper uncertainty range of the age model. The corrected couplet count extends to 1514 at a depth of 82.5 cm, underestimating the radiometrically modelled age at that depth (1470) by 44 years and extending 38 years beyond the upper uncertainty margin of the model (1552).

Sediment geochemistry

The sediments are largely composed of organic matter with TOC contents in the range of 16–33% (approximately 27–54% organic matter) and BSi contents between 23 and 57% (Fig. 4). XRF analysis revealed the main elemental components of the sediments, in addition to C, to be Si (19–29%), sulphur [S] (0.8–2.0%), calcium [Ca] (0.7–1.7%), iron [Fe] (0.4–1.4%) and aluminium [Al] (0.1–0.5%). BSi content shows a strong positive correlation with Si ($p < 0.01$) and strong negative correlations ($p < 0.01$) with TOC, TN, S and Ca and manganese [Mn]. Indicating allochthonous minerogenic input, the proportion of Titanium [Ti] increases threefold following a low in unit I, where it comprises around 0.01% of the sediments, and remains above 0.045% after a peak at 0.074% in unit V (around 1900; Fig. 4).

In unit I, TOC content shows maximum values in the range 29–33%, while BSi content shows minimum values in the range of 25–31%. Large changes in TOC and BSi contents occur from unit I to unit II, with a substantial reduction in TOC content to 17% and a twofold increase in BSi content to over 50%, mostly persisting to mid-unit III (late 1600s). From unit I to unit II, Si increases from 18 to 28%, concurrent with reductions in Ca (from 1.7 to 0.7%) and S (1.4 to 1.0%). The Fe/Ti ratio decreases by around 50% in unit I, followed by relatively stable values. At the transition from unit I to unit II (late 1400s) Ca and S abruptly decrease by around 60% and 30%, respectively, reflected by Ca/Ti and S/Ti, concurrent with an increase in K/Ti.

Unit III features a gradual increase in Ti to above 0.05%, over double its maximum in unit I. Following a sharp decline from 11.6 in unit I, C/N ratios recover in unit II and peak at 11.4 in unit III (around 1630). Throughout unit III, TOC and Si contents and the elemental ratios S/Ti, Ca/Ti and Fe/Ti show little variability and remain relatively stable.

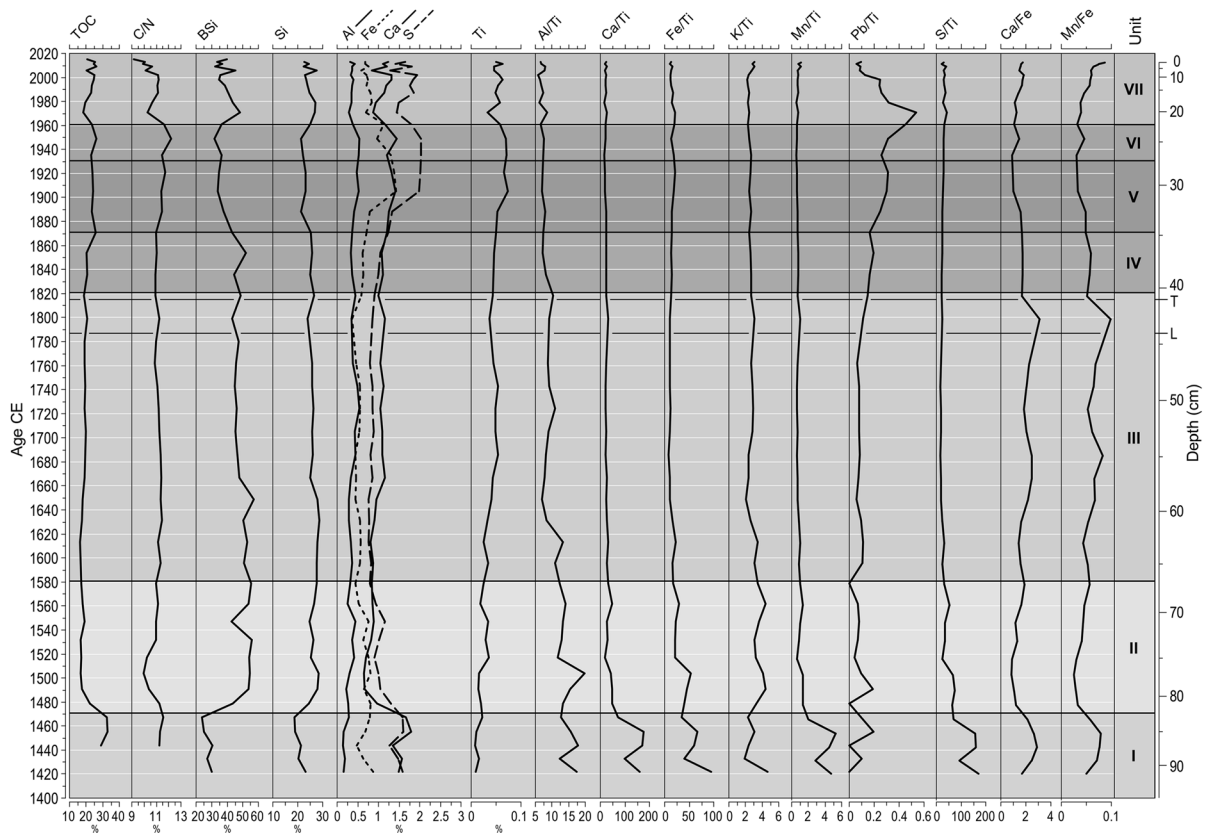


Fig. 4 Selected biogeochemical data. All variables are plotted against sediment age according to the age model shown in Fig. 2, with sediment depth shown to the right. Laki (1783–84) and Tambora (1815) are indicated by broken lines labelled L and T next to the depth axis. Lithostratigraphic units (right) are indicated with representative greyscale values based on

the averaged sediment colour of each unit. Left to right: total organic carbon (TOC) content, atomic C/N ratio, biogenic silica (BSi) content, XRF measurements of Si, Al, Fe, Ca, S and Ti, and derived elemental XRF ratios, constrained by Ti (Al, Ca, Fe, K and Pb) and Fe (Ca, Mn)

From unit IV (1820) TOC content abruptly increases and C/N ratios continue to increase through unit V. BSi content declines from around 48% in unit IV to around 35% in unit V, reflected by lower Si content in unit V. Sediments in units V and VI show similarity to those in unit I in terms of C/N ratios, BSi content, and several inorganic elements, although elevated Ti contents indicate greater allochthonous input. Along with an increase in Ti in units V and VI, S, Fe and Al continue to increase, exceeding their unit I values in unit VI (around 1950), where TOC content increases slightly along with C/N ratios, and BSi content declines to a low point. Unit VII (1960–2016) represents the poorly compacted top sediments, which are characterised by elevated variability in sediment composition. The C/N ratio

continues a declining trend from unit VI to its lowest value of 9.1 in unit VII. From the 1970s until the present, BSi content ranges between 32 and 48%, which represents a decline of around 20% compared to units II–IV (1480–1890).

Diatom assemblages

A total of 17 diatom species comprising at least 3% of the assemblage in at least one sample were identified (Fig. 5). Five diatom-community zones (D1–5) were defined, covering the following periods: D1 (1414–1502), D2 (1502–1640), D3 (1640–1772), D4 (1772–1955) and D5 (1955–2016). Planktonic species comprise at least 85% in all samples. Throughout the record, the diatom assemblage is characterised

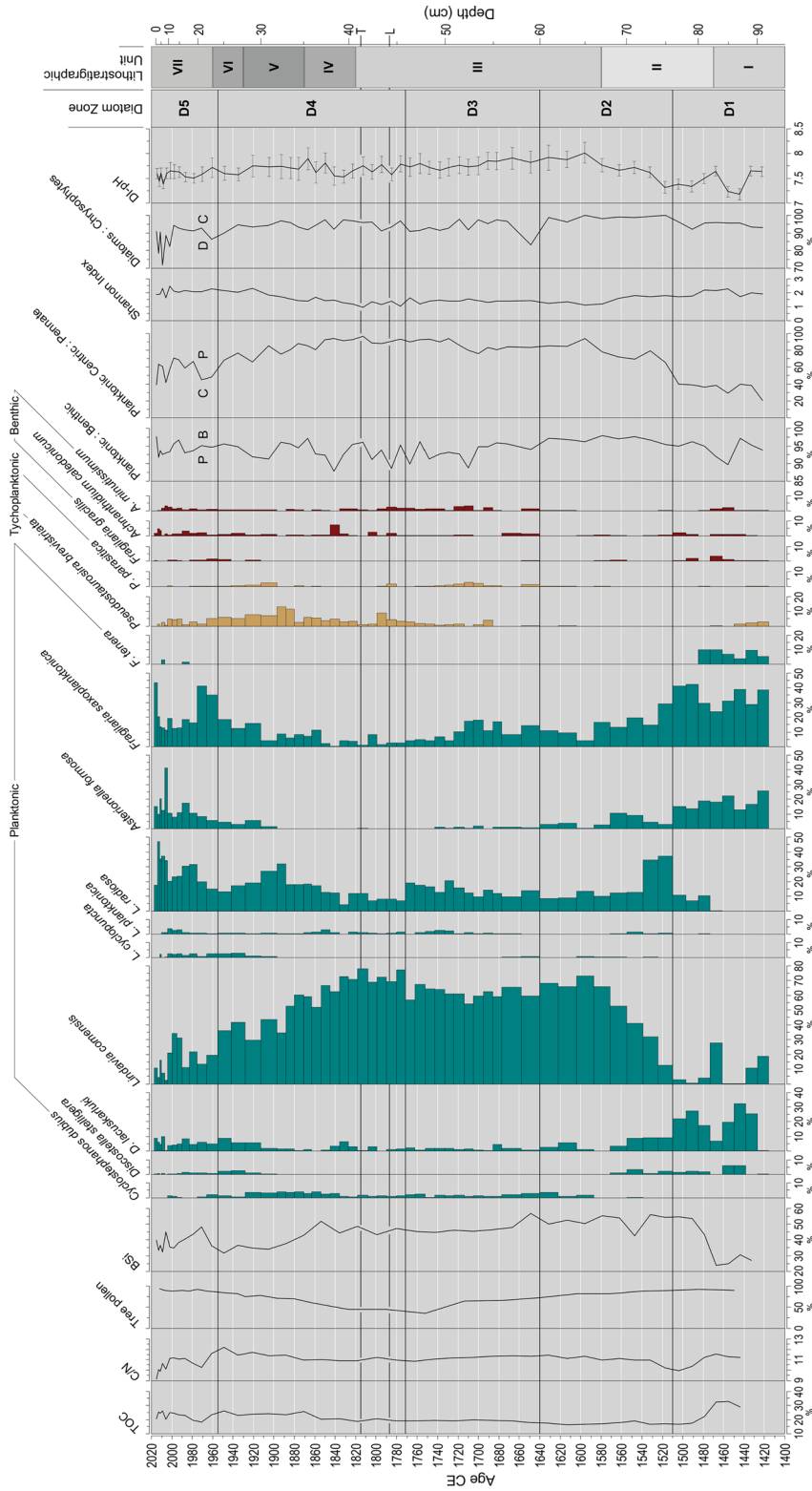


Fig. 5 Diatom stratigraphy and selected geochemical variables. All variables are plotted against sediment age according to the age model shown in Fig. 2. Diatom-community zones based on CONISS, lithostratigraphic units (Fig. 4) and corresponding sediment depths are shown to the right. Laki (1783–84) and Tambora (1815) are indicated by broken lines labelled L and T next to the depth axis. The diatom species shown comprise at least 3% of the assemblage in at least one sample. From left to right: total organic carbon (TOC) content, atomic C/N ratio, % tree pollen, adapted from (Damber 2020), biogenic silica (BSi) content, dominant diatom species sorted into planktonic (green), tycho planktonic (yellow) and benthic (red) groups, the relative proportions of Planktonic to Benthic diatoms and Centric and Pennate diatoms within the planktonic fraction of the assemblage, Shannon's diversity Index, and diatom-inferred pH (DI-pH) showing standard error margins

by combinations of *Lindavia comensis*, *L. radiosa*, *Fragilaria saxoplanktonica*, *A. formosa*, *Discostella lacus-karluki* (Fig. S2) and *Pseudostaurosira brevistriata* (Grunow). Only four benthic and two tycho-planktonic species are dominant, of which no species comprises more than 5% prior to D4. The proportion of diatoms to chrysophytes is generally high throughout the record, except in the most recent part (D5) where the relative proportion of chrysophytes increases as well as the variability.

Zone D1 consists largely of *A. formosa* (12–25%), *D. lacus-karluki* (up to 32%) and species of *Fragilaria* (37–45% with around two thirds consisting of *F. saxoplanktonica*). DI-pH indicates relatively neutral conditions throughout D1. As is the case throughout the record, the proportion of benthic species is low, remaining less than 14% in D1. In D1 the proportion of centric species within the plankton is low, consisting mostly of *D. lacus-karluki* and sporadically *L. comensis*, with *Lindavia radiosa* appearing in the late 1400s with a relative abundance of 10–20%.

In Zone D2 the contribution of *L. comensis* increases to over 65% in the late 1500s, over quadruple its contribution of around 12% in the early 1500s. This is accompanied by declining contributions of multiple species, most notably, *F. saxoplanktonica* and *D. lacuskarluki*. While the entire record is dominated by a few species, D2 contains the lowest contribution of benthic and tycho-planktonic species.

Zone D3 retains much of the assemblage structure of the later part of D2, with BSi content persisting above 40%. Until the mid-1600s *F. saxoplanktonica* is the only dominant pennate species consistently present. From around 1700 the proportion of tycho-planktonic species increases, with *P. brevistriata* establishing a minor component among the dominant species. An increase in alkalinity is indicated by DI-pH from around 1560, accompanied by greater uncertainties, which mostly persist through D3. *Asterionella formosa* contributes little to the assemblage in D3 and *F. saxoplanktonica* declines from 18 to 4% between 1700 and 1770.

Zone D4 marks a decline in *L. comensis* dominance, coinciding with a marked reduction in BSi content from ~50% in the mid 1800s to 30–35% between 1850 and 1900. In timing with the declining *L. comensis* dominance, other planktonic taxa (*F. saxoplanktonica* and *L. radiosa*) increase, collectively comprising a similar proportion of the assemblage

as *L. comensis* by the early 1900s. *Pseudostaurosira brevistriata* is more common in D4 than in any other zone, comprising 5–10%.

Zone D5 aligns closely with unit VII, which represents the topmost, poorly compacted sediments. From the late 1950s, the assemblage transitions to a composition resembling D1, albeit with *L. radiosa* frequently the most dominant species, followed by *F. saxoplanktonica*. The sample resolution increases from 8 to 2 years between 1950 and 2015, which contributes to the greater variability of some species including *L. comensis* (ranging from 3 to 34%, avg. 16%) and *A. formosa* (ranging from 8 to 41%, avg. 4%).

Differences in sediment composition over time

The principal component analysis (Fig. 6) illustrates the relationships between biogeochemical variables (BSi, TOC and TN contents and other major XRF-based element counts) and the similarity of 37 samples at 2–80 cm depth along the first two axes. The first four components explain 87% of the variation among the geochemical data, with 71% explained by the first two components. The first principal component (PC1) represents the sediment composition, separating BSi and Si from TOC and other elements. The separation of Si from all other elements and its alignment with BSi suggests that most of the silica in the sediments is biogenic in origin, supported by a strong positive correlation between BSi and Si (Pearson's Correlation Coefficient=0.9). PC2 separates elements commonly associated with minerogenic input and weathering (Rb, Al, K, Ca, Ti) from elements associated with redox conditions, soluble compounds or pedogenic processes (Cu, P, Ni, Fe, S). On PC2, Ca is separated from other elements commonly belonging to minerals of authigenic origin (Fe, S), aligning closely with K, Ti and Mn.

While the PCA did not involve any diatom data, the plot of PC1 against PC2 shows some clustering of the samples belonging to separate diatom zones. D1 is loosely associated with BSi and Si on PC1 and away from minerogenic variables on PC2. Both D2 and D3 are also associated with silica variables on PC1, with D3 samples grouped away from typically more mobile variables on PC2. D4 and D5 lack strong associations with BSi and Si on PC1, with D4 associated more with TOC and D5 associated both

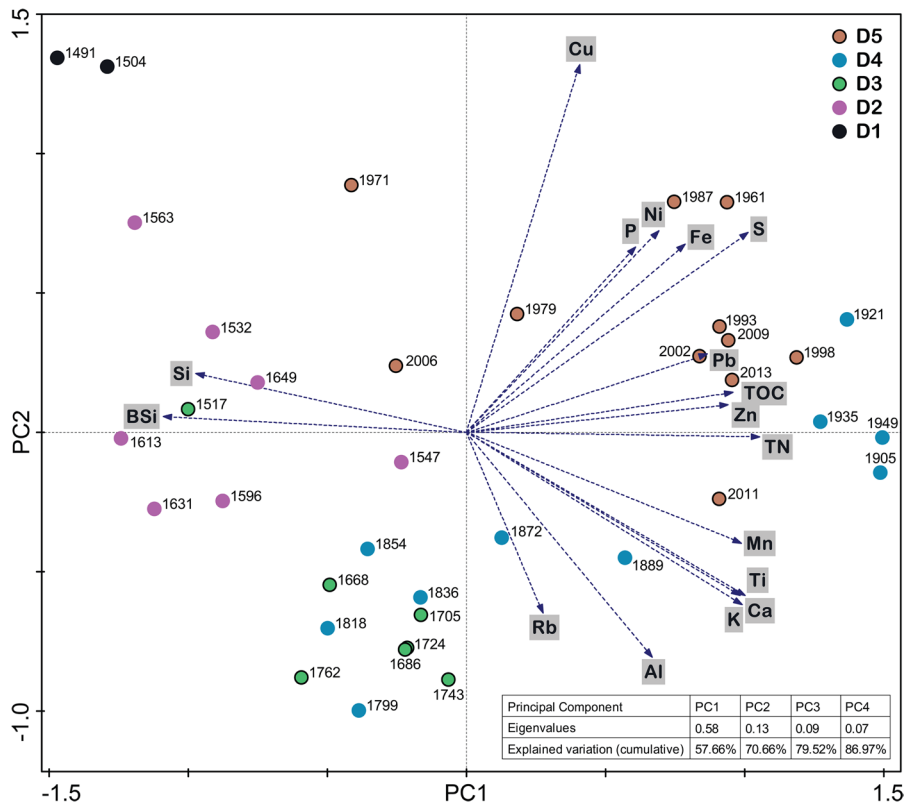


Fig. 6 Biplot of the first and second principal components of a PCA of geochemical data, including TOC, TN, BSi and multiple XRF-based element counts (Si, Cu, P, Ni, Fe, S, Pb, Zn, Mn, Ca, Ti, K, Al and Rb). Variables are indicated by arrows and samples by points. While no diatom data were used in the PCA, sample points are coloured to indicate the diatom zones (D1-D5; Fig. 5) from which the geochemical data were obtained, indicated to the top right. Eigenvalues and explained

variations of the first four principal components are shown to the bottom right. A sensitivity analysis was first performed with and without Si and BSi to ensure that the inclusion of both variables did not significantly influence the principal components and the explained variations. The first four principal components explain 87% of the variation among the data. Together, PC1 and PC2 explain 71% of the variation

with typically more mobile elements and with TOC and Pb.

Discussion

Varve formation and diatom seasonality

Our combined diatom, EDS, and SEM data show that the recent sediments of Odensjön contain annually deposited couplets of light (spring through autumn) and dark (late autumn through spring) laminae, forming varves of a predominantly biogenic composition (Fig. 3). A well-defined clastic component is absent, mainly owing to the lack of fine-grained deposits in the lake catchment (Fig. 1). The components of

biogenic varves depend on factors such as in-lake productivity, nutrient loading and detrital organic matter input (Zolitschka et al. 2015). Our EDS results show greater amounts of Si and O in the lighter summer laminae, largely representing diatom frustules, as confirmed by SEM. A greater proportion of C, mostly representing organic matter which falls out of suspension in winter, combined with fewer diatom frustules, results in the darker appearance of the winter laminae. Ca is a minor component of the sediments overall (Figs. 3b, 4) and although carbonate clasts are absent in the glaciofluvial deposits northeast of the lake (Ringberg 1984), the greater proportion of Ca in the dark laminae likely originates from minor amounts of Ca-bearing detrital mineral matter transported from the catchment during autumn and winter.

Diatom species associated with either light or dark laminae in the top sediments (Fig. 3a) include *L. comensis*, *L. radiosa* and *A. formosa*, which commonly co-exist in temperate and boreal lakes and are frequently associated with seasonal changes, including turnover timing, the degree of mixing and nutrient availability, and the presence and timing of winter ice cover (Sivarajah et al. 2016; Edlund et al. 2022). In the top sediments, each dark lamina contains a greater proportion of centric species in the planktonic fraction, including *L. radiosa* and *L. comensis*, with each underlying light lamina dominated by *A. formosa*. The latter is commonly associated with nutrient enrichment (Saros et al. 2005) and typically blooms when thermal stratification is poor in spring and autumn (Garibaldi et al. 2003; Feuchtmayr et al. 2012) but can persist into the summer if thermal stratification is poor and nutrients, particularly N, are in sufficient supply (Malik et al. 2018). *Lindavia comensis* is a common member of the deep plankton in circumneutral to alkaline lakes (Bennion and Simpson 2011), frequently blooms during late summer to autumn in temperate climates (Reavie et al. 2017) and is positively associated with elevated epilimnetic temperatures (Malik and Saros 2016; Ossyssek et al. 2020; Szczerba et al. 2023). *Lindavia radiosa* is a largely cosmopolitan species with generally high light requirements (Saros et al. 2014; Malik and Saros 2016) and is resilient under P limitation (Malik et al. 2017). *Fragilaria saxoplanktonica* comprises at least 10% and does not exhibit an affinity to either type of lamina. Reports of *D. lacus-karluiki* are infrequent and this species is likely to have been widely reported as *D. pseudostelligera* Hustedt, *D. stelligera* Cleve & Grunow, or other small taxa, such as *D. glomerata* Bachmann (Potapova et al. 2020). Here *D. lacuskarluiki* only bloomed during one of the years in the top sediments, presumably due to preferable conditions through autumn.

We propose the following annual diatom succession in Odensjön. Supported by an influx of nutrients during snowmelt, *A. formosa* dominates the spring assemblage and persists throughout the summer. Conditions for colony suspension probably remain favourable during summer, in support of *A. formosa*, as the north-facing back-wall of the catchment and shading provided by forest cover may result in delayed warming and prolonged circulation in the epilimnion. *Asterionella formosa* then begins to decline and fall out of

suspension, probably together with other planktonic material as nutrients are depleted and surface temperature rises. This results in reduced turbidity of the epilimnion, which benefits centric species requiring greater light penetration. Among these, *L. comensis* also benefits from warming of the epilimnion, and *L. radiosa* continues its growth as nutrients become depleted in late summer. The relative abundance of *A. formosa* and *F. saxoplanktonica* in the dark laminae suggests that nutrient availability and circulation in the epilimnion remains sufficient to support their persistence through the colder months.

In recent decades the light laminae are dominated by *A. formosa* and *F. saxoplanktonica*. While observations of *A. formosa* are common, frequently highlighting its increasing dominance in the Northern Hemisphere likely because of recent warming, observations of *F. saxoplanktonica* are less frequent, although it is likely that it follows the general trend of fragiliarioid species in response to warming and nutrient enrichment, including that of atmospheric nitrogen (Saros et al. 2005).

The surface waters of Odensjön commonly freeze during the winter. However, the proportion of benthic diatoms appears to lack a relationship to summer or winter laminae (Fig. 3a), which may indicate that the spring ice-melt has a limited impact on mixing and circulation of the epilimnion. In addition, rapid-blooming species are present in the modern assemblage, including *F. saxoplanktonica* and *A. formosa*. These species are highly competitive in early spring and late autumn (Wang et al. 2012) and their relative abundances probably obscure signs of increased benthic productivity, which may occur following spring ice-melt and nutrient influx. The proportion of planktonic to benthic diatoms is also dependent on the available planktonic and benthic habitat in relation to the coring location (Stone and Fritz 2004). Despite its small size, the steep bathymetry probably leads to underrepresentation of benthic diatom species in Odensjön's deep sediments where varves are present, like in other small lakes (Anderson et al. 1994).

At inter-annual timescales, increased relative abundances of chrysophyte cysts have been associated with lowered temperatures and nutrient depletion during autumn and winter (Firsova et al. 2008). While chrysophytes can be associated with ice-off timing (Agbeti and Smol 1995), the ratio of diatoms to chrysophytes does not show any significant

difference between summer and winter laminae at present (Fig. 3a). This could suggest more complex or successive chrysophyte production periods, which are not revealed by raw counts. In addition, the absence of seasonal chrysophyte dynamics may be expected, as chrysophytes are a more ubiquitous indicator of temperature and climate over longer periods (Smol 1985).

Lake and catchment development since the early 1400s

Our sediment record extends back to the early 1400s, when the landscape on the Söderåsen Horst was dominated by *Fagus* and pasture according to pollen records from two small peatlands nearby Skärälid, approximately 4 km North of Odensjön (Bergman 2000). The previously heavily forested landscape of southern Sweden was affected by increased openness due to human expansion from around 3000 cal. yrs BP. However, at the onset of our record the region was undergoing extensive regrowth of forest in peripheral areas, such as the Söderåsen Horst, following a marked population decline in Late Medieval times related to the Black Death (Berglund et al. 2008; Lagerås 2013).

The most abrupt shift in the diatom assemblage occurred from the late 1400s through to the mid-1500s (Fig. 5) with a transition from an assemblage mostly dominated by pennates (*A. formosa* and *F. saxoplanktonica*) to one overwhelmingly dominated by centrics (*L. comensis* and *L. radiosa*). Emerging in the late 1400s, *L. comensis* became the dominating taxon in the mid-1500s and maintained its status through to the late 1800s. The reductions in TOC content and C/N ratio from the late 1400s indicate a declining contribution of organic matter from the surrounding catchment, partly explaining the concurrent relative increase in BSi content of the sediments. This is seen in the PCA (Fig. 6) in which D2 is associated with BSi along PC1. The importance of light availability and mixing in the epilimnion for both *L. comensis* and *L. radiosa* points to a relationship with a concurrent decline in tree pollen from the mid-1500s, peaking in the 1800s in response to a major agrarian expansion (Lagerås 2013). This development is evidenced by pollen and macrofossil data from the same sediment record (Damber 2020), where *Fagus* macrofossils (buds, leaves and leaf fragments) are notably

absent from 1750 to 1900. It is likely that reduced forest cover near the lake margins improved the light availability to the benefit of *L. radiosa*, and exposed the surface waters to wind shear, improving circulation in the epilimnion to the benefit of *L. comensis*. Likewise, reduced light availability and circulation associated with the return of forest cover explains the decline of *L. comensis* from the late 1800s and the returning contribution of pennate species in the planktonic fraction of the assemblage.

In recent decades the diatom assemblage largely resembles that of the 1400s, although *D. lacuskarluiki* is replaced by *L. radiosa*. Recent studies show an increasing abundance of small species of *Discostella* in warming regions with declining periods of ice cover (Panizzo et al. 2013). Small cyclotelloid species including *Discostella* and *Lindavia* can outcompete other species in well-stratified temperate lakes (Rühland et al. 2008; Saros and Anderson 2015; Stone et al. 2016). While increases in *Discostella* are often attributed to elevated concentrations of dissolved organic carbon (DOC), as observed in other recent lake records from southern Sweden (Bragée et al. 2015), it is probable that *L. radiosa* now fills this niche in Odensjön, because it is reported to have an elevated DOC optimum (Rühland et al. 2003). Recent decades show a decline in *L. comensis*, accompanied by increasing contributions of *F. saxoplanktonica* and *A. formosa* as widely documented elsewhere in recent decades (Sivarajah et al. 2016). The recent prominence of *A. formosa* is probably related to earlier ice-off timing and longer ice-free periods because this species commonly blooms during the spring (Feuchtmayr et al. 2012) and is particularly competitive in low nutrient environments in warming regions (Sivarajah et al. 2016). From the late 1700s the tycho planktonic species *P. brevistriata* also became dominant. Observations of this species in cold, oligotrophic environments indicates that it has a circumneutral optimum (Cameron et al. 1999; Rosén et al. 2000; Bigler et al. 2000), and it is also known to have a wide range of environmental tolerances including input of allochthonous organic matter (Wunsam et al. 1999; Cantonati et al. 2009). Its establishment here is likely related to increased nutrient availability (Cantonati et al. 2021). Similarly, the high frequencies of *A. formosa*, *F. saxoplanktonica* and *P. brevistriata* in recent decades, coinciding with the re-establishment of forest, probably reflect increased

supply of nutrients from leaf litter on the talus slopes surrounding the lake. Recent atmospheric N deposition (Bergström and Jansson 2006) is likely to also have benefitted both *A. formosa* and *F. saxoplanktonica* (Saros et al. 2005).

The catchment is presently dominated by *Fagus sylvatica*, which re-established in the late 1800s after having been largely absent, as indicated by macrofossil data from Odensjön and tree-ring records from its margins (Damber 2020). The establishment of *Fagus* has been shown to result in soil acidification (Achilles et al. 2021), resembling the more commonly observed effects of *Picea* establishment (Augusto et al. 2002), although the effects of their respective establishment on soil nutrient and cation availability are complex (Diers et al. 2021). Both K/Ti and Al/Ti ratios indicate relatively stable weathering conditions in the catchment during recent centuries (Fig. 4) and DI-pH shows limited variations, remaining mildly alkaline despite significant changes in the diatom assemblage since the mid-1800s (Fig. 5). As supported by recent pH measurements in the range of 7.1–7.3, these observations suggest relatively high buffering capacity in the catchment, providing resilience to the potential acidifying effects of forest regrowth, although the slight minimum in DI-pH around 1980 may reflect the well-documented peak in airborne S deposition from fossil fuel combustion at the time (Sverdrup et al. 2005). More generally, the assumed increase in nutrient supply from forest recovery and industrialisation probably benefitted the dominant diatom species.

The darkest sediments of units V and VI, which date to between 1870 and 1960, are the result of a 30% decline in BSi content associated with diatom productivity (Fig. 4). In the early 1900s, increasing allochthonous input, indicated by rising Ti content, resulted in both the Fe/Ti and S/Ti ratios partly obscuring the notable 100% increase in both Fe and S content. Despite the decline in BSi content, the loss of organic matter contributed by diatoms was replaced by a relatively larger supply of allochthonous organic matter from the catchment, indicated by increasing C/N ratios and TOC content. This is clearly corroborated by the increase in tree pollen in the 1900s and the abundance of leaves in units VI and VII (Fig. 2, Table 1). The Mn/Fe ratio, which is commonly used as an indicator of oxygenation of the hypolimnion (Melles et al. 2012), suggests that dissolved oxygen concentrations declined markedly from a high in

the late 1400 s, then increased gradually from about 1500 to 1800, followed by an abrupt decline in the early 1800s and a gradual increase until the present (Fig. 4). Hence, the Mn/Fe ratio broadly represents variably favourable conditions for the preservation of varves, with near absence in unit I, although constraints on the diatom productivity and associated complications for counting of varves were caused by forest expansion and the massive occurrence of leaves in the uppermost units (Fig. 2, Table 1). Throughout the record, the alignment of the Ca/Fe and Mn/Fe ratios primarily reflects variations in Fe content. The Ca/Fe ratio has been associated with weathering of catchment soils and pedogenic input (Elbert et al. 2013). From the early 1800s both Ca and Mn contents increase relative to Ti, albeit to a lesser extent than Fe, resulting in declining Mn/Fe and Ca/Fe ratios. The differential mobilisation of Ca and Mn relative to Fe may be related to a strengthened hypolimnetic oxygen deficit.

The changes in sediment delivery and aquatic environment related to catchment dynamics as described above probably contributed strongly to the pronounced variations in preservation and associated possibilities of accurate counting of varves in the sediments of Odensjön (Fig. 2). Although our comparison of extended varve counting and radiometric dating of the sediment record indicates underestimation of varve-based ages below about 30 cm depth, alternative explanations cannot be excluded. As shown by for example Bonk et al. (2015), radiocarbon dates obtained on varved sediments may yield too old ages because of fluvial redeposition of terrestrial plant remains from catchment soils. However, given the very restricted catchment of Odensjön and its lack of well-defined inflowing streams, we consider it more likely that the deviating age determinations reflect larger amounts of missing varves in the uncountable sections than represented by our attempt at correcting the varve count based on interpolation.

Diatom-inferred pH and the potential impacts of major volcanic eruptions

Despite significant shifts in diatom assemblage structure, DI-pH fluctuates in the range of 7.1–8.0 throughout the record, the most significant change being an increase of around 1 pH unit during the 1500 s (Fig. 5). This inferred shift towards increased

alkalinity probably reflects enhanced base saturation related to agricultural expansion (Renberg et al. 1993; Rosén and Hammarlund 2007), although reduced diatom diversity may have contributed. At this stage, *L. comensis*, with a pH optimum of 8–9 (Ossyssek et al. 2020) increased in dominance largely in response to decreasing forest cover. The relatively invariable DI-pH record, remaining around 7.5–8 in recent centuries despite large variations in both local land use and regional acid deposition, indicates relatively high buffering capacity in the catchment as compared to other lakes in the region (Renberg et al. 1993). In contrast to DI-pH, the effects of land-use dynamics around Odensjön, as well as regional environmental changes related to industrialization are sensitively recorded by variations in BSi content and centric to pennate diatom ratios (Fig. 5). According to our results and recent pH measurements, the waters of Odensjön remain mildly alkaline under well-buffered conditions at present and were therefore likely to have been relatively resilient to acid deposition in the past. Hence, the potential impact of S deposition following the eruption of Laki 1783–84 may have been short-lived given the acute nature of the event (Thordarson and Self 2003).

Given the complications of counting varves beyond about 1900, any evaluation of the potential effects of older external forcings of known age must be partly speculative, although we consider this motivated for the targeted volcanic eruptions in the upper part of our highly resolved record where the uncertainty of the age model is relatively low (Fig. 2). The openness of the catchment persisted throughout the period encompassing both Laki 1783–84 and Tambora 1815 (Fig. 5). In combination with relatively invariable climatic conditions in southern Sweden at the time (Edwards et al. 2017), we can assume largely stable background conditions against which the impacts of S deposition (Laki) and hydroclimatic extremes (Tambora) may be determined. However, the dominance of *L. comensis* is problematic as it seemingly elevates the uncertainties of DI-pH within the period of about 1600–1920 (Fig. 5). Nevertheless, the slight decrease in DI-pH recorded in the sample dated to 1780–1790, which ranks as the third lowest pH and the second lowest uncertainty within the period of large uncertainties in DI-pH (1600–1920), could potentially represent a local response to the Laki acid deposition event. A shift towards reduced oxygen deficit in the

hypolimnion is indicated by the elevated Mn/Fe ratio of the sediment sample postdating Laki, followed by a return to previous levels around 1820, in timing with the eruption of Tambora (Fig. 4). There is little change in the diatom community immediately following the eruption of Tambora, and changes in the diatom community in the 1800s are largely explained by the return of forest cover at the lake edge, which limits the possibility of assessing the potential climatic impacts of Tambora.

Conclusions

Odensjön's varved sediment record offers great potential for highly resolved paleoenvironmental studies based on more extended sampling than in the present study. Such records are also needed to assess the extent to which the composition of the diatom assemblage of the early 1400 s characterises typical conditions at the site prior to the following deforestation. Our oldest adjusted varve age underestimates the sediment age by 44 years versus the radiometrically based age model, while extending 38 years beyond the model's upper uncertainty margin. The sediments contain beds where the biogenic varves are poorly distinguishable, primarily from the period of maximum land-use intensity in the late 1800s. Varve counting is also complicated by the low amount of minerogenic matter in the sediments, which leads to very thin varves following compaction. Improvements to the varve record should be sought in future studies using additional methods for varve inspection (e.g. thin section analysis, XRF elemental mapping and X-ray imaging).

Our results show that the diatom assemblage was relatively stable during much of the Little Ice Age (LIA), a period of increased epilimnetic circulation and enhanced light availability associated with a general decline in sheltering forest cover. The diatom succession appears to be heavily dependent on changes associated with forest cover, illustrated by the clear shift from a pennate- to a centric-dominated planktonic fraction of the assemblage as forest cover declined in the 1500 s and some reversal as forest cover returned from the late 1800s (Fig. 5). In addition to these anthropogenic forcings, direct climatic effects of the LIA, primarily in the form of an extended ice-cover season, probably contributed to

the observed dynamics. The diatom community was heavily dominated by *Lindavia comensis* throughout the period encompassing the eruptions of Laki in 1783–84 and Tambora in 1815. Our DI-pH reconstruction potentially indicates minor acidification of Odensjön immediately following the eruption of Laki. Changes in sediment chemistry following the timing of Tambora appear to be related to redox conditions associated with the re-establishment of forest cover, providing no evidence of regional climate effects of the eruption.

To our knowledge this is the first Scandinavian report of *Discostella lacuskarluki* amongst the dominant species in an assemblage, although as highlighted by Potapova et al. (2020), this small taxon is easily overlooked and is likely to have been reported as similar taxa. The identification was confirmed by SEM (Fig. S2).

Acknowledgements This study was funded by grants from the Swedish Research Council (2017-03698) to Dan Hammarlund and the Royal Physiographic Society in Lund (nr. 40986) to Ethan Silvester. We are grateful to Mats Rundgren for his comments on the manuscript and to Yevhenii Rohozin for participating in the fieldwork and preparing the illustration of Fig. 1. Two anonymous reviewers provided valuable comments on the manuscript.

Author contributions ELS wrote the main manuscript text. DH, KL and RB reviewed and improved the manuscript. All authors contributed to the geochemical analyses. Diatom analysis was performed by ELS. ELS prepared all figures and tables, with the exception of Fig. 1. All authors reviewed the manuscript.

Funding Open access funding provided by Lund University, Royal Physiographic Society of Lund, 40986, Vetenskapsrådet, 2017-03698

Data availability Data are available from the corresponding author upon reasonable request.

Declarations

Conflict of interest The authors declare no competing interests.

Open Access This article is licensed under a Creative Commons Attribution 4.0 International License, which permits use, sharing, adaptation, distribution and reproduction in any medium or format, as long as you give appropriate credit to the original author(s) and the source, provide a link to the Creative Commons licence, and indicate if changes were made. The images or other third party material in this article are included in the article's Creative Commons licence, unless indicated otherwise in a credit line to the material. If material is not

included in the article's Creative Commons licence and your intended use is not permitted by statutory regulation or exceeds the permitted use, you will need to obtain permission directly from the copyright holder. To view a copy of this licence, visit <http://creativecommons.org/licenses/by/4.0/>.

References

- Achilles F, Tischer A, Bernhardt-Römermann M, Heinze M, Reinhardt F, Makeschin F, Michalzik B (2021) European beech leads to more bioactive humus forms but stronger mineral soil acidification as Norway spruce and Scots pine—results of a repeated site assessment after 63 and 82 years of forest conversion in central Germany. *For Ecol Manage* 483:118769
- Agbeti MD, Smol JP (1995) Chrysophyte population and encystment patterns in two Canadian lakes. *J Phycol* 31:70–78
- Anderson NJ, Korsman T, Renberg I (1994) Spatial heterogeneity of diatom stratigraphy in varved and non-varved sediments of a small, boreal-forest lake. *Aquat Sci* 56:40–58
- Appleby PG (2001) Chronostratigraphic techniques in recent sediments. In: Last WM, Smol JP (eds) *Tracking environmental change using lake sediments: basin analysis, coring, and chronological techniques*. Springer, Netherlands, Dordrecht, pp 171–203
- Arnaud F, Révillon S, Debret M, Revel M, Chapron E, Jacob J, Giguet-Covex C, Poulénard J, Magny M (2012) Lake Bourget regional erosion patterns reconstruction reveals Holocene NW European Alps soil evolution and paleohydrology. *Quatern Sci Rev* 51:81–92
- Augusto L, Ranger J, Binkley D, Rothe A (2002) Impact of several common tree species of European temperate forests on soil fertility. *Ann for Sci* 59:233–253
- Balkanski Y, Menut L, Garnier E, Wang R, Evangeliou N, Jourdain S, Eschstruth C, Vrac M, Yiou P (2018) Mortality induced by PM 2.5 exposure following the 1783 Laki eruption using reconstructed meteorological fields. *Sci Rep* 8(1):15896
- Battarbee RW, Juggins S, Gasse F, Anderson NJ, Bennion H, Cameron NG, Ryves DB, Pailles C, Chalié F, Telford R (2001) European diatom database (EDDI). An information system for palaeoenvironmental reconstruction. ECRC research report No 81, University College London, p 94
- Battarbee RW, Renberg I (1990) The surface water acidification project (SWAP) Palaeolimnology programme. *Philos Trans R Soc Lond* 327:227–232
- Bennion H, Simpson GL (2011) The use of diatom records to establish reference conditions for UK lakes subject to eutrophication. *J Paleolimnol* 45:469–488
- Berglund BE, Rapp A (1988) Geomorphology, climate and vegetation in north-west Scania, Sweden, during the Late Weichselian. *Geogr Pol* 55:13–35
- Berglund BE, Gaillard MJ, Björkman L, Persson T (2008) Long-term changes in floristic diversity in southern Sweden: Palynological richness, vegetation dynamics and land-use. *Veg Hist Archaeobotany* 17(5):573–583

- Bergman J (2000) Skogshistoria i Söderåsens nationalpark: en pollenanalytisk studie i Söderåsens nationalpark, Skåne. MSc. thesis no. 119, Department of Geology, Lund University.
- Bergström A-K, Jansson M (2006) Atmospheric nitrogen deposition has caused nitrogen enrichment and eutrophication of lakes in the northern hemisphere. *Glob Chang Biol* 12:635–643
- Bigler C, Hall RI, Renberg I (2000) A diatom-training set for palaeoclimatic inferences from lakes in northern Sweden. *SIL Proc* 1922–2010(27):1174–1182
- Blaauw M, Christen JA, Lopez MAA, Vazquez JE, Gonzalez V, Belding T, Theiler J, Gough B, Karney C (2021) Package ‘rbacon’.
- Bonk A, Tylmann W, Goslar T, Wacnik A, Grosjean M (2015) Comparing varve counting and ^{14}C -AMS chronologies in the sediments of Lake Żabińskie, Northeastern Poland: implications for accurate ^{14}C dating of lake sediments. *Geochronometria* 42(1):159–171
- Bonk A, Piotrowska N, Zarczyński M, Enters D, Makohonienko M, Rzodkiewicz M, Tylmann W (2023) Limnological responses to environmental changes during the last 3,000 years revealed from a varved sequence of Lake Lubiąskie (western Poland). *Catena* 226:107053
- Bragée P, Mazier F, Nielsen AB, Rosén P, Fredh D, Broström A, Granéli W, Hammarlund D (2015) Historical TOC concentration minima during peak sulfur deposition in two Swedish lakes. *Biogeosciences* 12(2):307–322
- Brännvall ML, Kurkkio H, Bindler R, Emteryd O, Renberg I (2001) The role of pollution versus natural geological sources for lead enrichment in recent lake sediments and surface forest soils. *Environ Geol* 40:1057–1065
- Brönnimann S, Krämer D (2016) Tambora and the “Year Without a Summer” of 1816. A perspective on earth and human systems science (Vol. 90). *Geographica Bernensia*
- Cameron NG, Birks HJB, Jones VJ, Berges F, Catalan J, Flower RJ, Garcia J, Kawecka B, Koinig KA, Marchetto A, Sánchez-Castillo P (1999) Surface-sediment and epilithic diatom pH calibration sets for remote European mountain lakes (AL: PE Project) and their comparison with the Surface Waters Acidification Programme (SWAP) calibration set. *J Paleolimnol* 22:291–317
- Cantonati M, Scola S, Angeli N, Guella G, Frassanito R (2009) Environmental controls of epilithic diatom depth-distribution in an oligotrophic lake characterized by marked water-level fluctuations. *Eur J Phycol* 44(1):15–29
- Cantonati M, Zorza R, Bertoli M, Pastorino P, Salvi G, Platania G, Prearo M, Pizzul E (2021) Recent and subfossil diatom assemblages as indicators of environmental change (including fish introduction) in a high-mountain lake. *Ecol Ind* 125:107603
- Collins TJ (2007) ImageJ for microscopy. *Biotechniques* 43:25–30
- Conley DJ, Schelske CL (2001) Biogenic Silica. In: Smol JP, Birks HJB, Last WM et al (eds) *Tracking environmental change using lake sediments: terrestrial, algal, and siliceous indicators*. Springer, Netherlands, Dordrecht, pp 281–293
- Damber M (2020) A palaeoecological study of the establishment of beech forest in Söderåsen National Park, southern Sweden. <https://lup.lub.lu.se/student-papers/record/9033035/file/9033256.pdf>. Accessed 12 Sep 2023
- DeMaster DJ (1981) The supply and accumulation of silica in the marine environment. *Geochim Cosmochim Acta* 45:1715–1732
- Diers M, Weigel R, Culmsee H, Leuschner C (2021) Soil carbon and nutrient stocks under scots pine plantations in comparison to European beech forests: a paired-plot study across forests with different management history and precipitation regimes. *Forest Ecosyst* 8:47
- Dixit SS, Smol JP, Kingston JC, Charles DF (1992) Diatoms: powerful indicators of environmental change. *Environ Sci Technol* 26(1):22–33
- Dubois N, Saulnier-Talbot É, Mills K, Gell P, Battarbee R, Bennion H, Chawchai S, Dong X, Francus P, Flower R, Gomes DF (2018) First human impacts and responses of aquatic systems: a review of palaeolimnological records from around the world. *Anthrop Rev* 5(1):28–68
- Edlund MB, Ramstack Hobbs JM, Heathcote AJ, Engstrom DR, Saros JE, Strock KE, Hobbs WO, Andresen NA, VanderMeulen DD (2022) Physical characteristics of northern forested lakes predict sensitivity to climate change. *Hydrobiologia* 849(12):2705–2729
- Edwards TWD, Hammarlund D, Newton BW, Sjolte J, Linderson H, Sturm C, Amour NAS, Bailey JNL, Nilsson AL (2017) Seasonal variability in northern hemisphere atmospheric circulation during the medieval climate anomaly and the little ice age. *Quat Sci Rev* 165:102–110
- Elbert J, Wartenburger R, von Gunten L, Urrutia R, Fischer D, Fujak M, Hamann Y, Greber ND, Grosjean M (2013) Late Holocene air temperature variability reconstructed from the sediments of Laguna Escondida, Patagonia, Chile (45° 30' S). *Palaeogeogr Palaeoclimatol Palaeoecol* 369:482–492
- Feuchtmayr H, Thackeray SJ, Jones ID, De Ville M, Fletcher J, James B, Kelly J (2012) Spring phytoplankton phenology—patterns and drivers of change consistent among lakes in the same climatological region? *Freshw Biol* 57(2):331–344
- Firsova AD, Kuzmina AE, Tomberg IV, Potemkina TG, Likhoshway YV (2008) Seasonal dynamics of chrysophyte stomatocyst formation in the plankton of Southern Baikal. *Biol Bull* 35:507–514
- Garibaldi L, Anzani A, Marieni A, Leoni B, Mosello R (2003) Studies on the phytoplankton of the deep subalpine Lake Iseo. *J Limnol* 62(2):177–189
- Godlund S (1951) Djupkarta över Odensjön. SGÅ Lund
- Grattan J, Charman DJ (1994) Non-climatic factors and the environmental impact of volcanic volatiles: implications of the Laki fissure eruption of AD 1783. *Holocene* 4:101–106
- Hertzman H (2021) Odensjön—A new varved lake sediment record from southern Sweden. <https://lup.lub.lu.se/student-papers/record/9050993>. Accessed 15 Jan 2024
- Kahlert M, Kelly MG, Mann DG, Rimet F, Sato S, Bouchez A, Keck F (2019) Connecting the morphological and molecular species concepts to facilitate species identification within the genus *Fragilaria* (Bacillariophyta). *J Phycol* 55(4):948–970
- Komada T, Anderson MR, Dorfmeier CL (2008) Carbonate removal from coastal sediments for the determination of

- organic carbon and its isotopic signatures, $\delta^{13}\text{C}$ and $\Delta^{14}\text{C}$: comparison of fumigation and direct acidification by hydrochloric acid. *Limnol Oceanogr Methods* 6:254–262
- Lagerås P (2013) Medieval colonization and abandonment in the south Swedish uplands: a review of settlement and land use dynamics inferred from the pollen record. *Archaeologia Baltica* 20:77–90
- Lange-Bertalot H, Hofmann G, Werum M, Kelly M, Cantonati M (2017) Freshwater benthic diatoms of Central Europe: over 800 common species used in ecological assessment (Vol. 942, pp. 1–908). Schmittgen-Oberreifenberg: Koeltz Botanical Books.
- Linderholm HW, Nicolle M, Francus P, Gajewski K, Helama S, Korhola A, Solomina O, Yu Z, Zhang P, D'Andrea WJ, Debret M (2018) Arctic hydroclimate variability during the last 2000 years: current understanding and research challenges. *Climate Past* 14(4):473–514
- Malik HI, Saros JE (2016) Effects of temperature, light and nutrients on five *Cyclotella sensu lato* taxa assessed with in situ experiments in arctic lakes. *J Plankton Res* 38:431–442
- Malik HI, Northington RM, Saros JE (2017) Nutrient limitation status of Arctic lakes affects the responses of *Cyclotella sensu lato* diatom species to light: implications for distribution patterns. *Polar Biol* 40:2445–2456
- Malik HI, Warner KA, Saros JE (2018) Comparison of seasonal distribution patterns of *Discostella stelligera* and *Lindavia bodanica* in a boreal lake during two years with differing ice-off timing. *Diatom Res* 33:1–11
- Melles M, Brigham-Grette J, Minyuk PS, Nowaczyk NR, Wennrich V, DeConto RM, Anderson PM, Andreev AA, Coletti A, Cook TL, Haltia-Hovi E (2012) 28 million years of Arctic climate change from Lake El'gygytyn. NE Russia. *Sci* 337(6092):315–320
- Nakov T, Guillory W, Julius M, Theriot E, Alverson A (2015) Towards a phylogenetic classification of species belonging to the diatom genus *Cyclotella* (Bacillariophyceae): transfer of species formerly placed in *Puncticulata*, *Handmannia*, *Pliocaenicus* and *Cyclotella* to the genus *Lindavia*. *Phytotaxa* 217(3):249–264
- Ojala AEK, Saarinen T, Salonen V (2000) Preconditions for the formation of annually laminated lake sediments in southern and central Finland. *Boreal Environ Res* 5(3):243–255
- Oppenheimer C (2003) Climatic, environmental and human consequences of the largest known historic eruption: Tambora volcano (Indonesia) 1815. *Prog Phys Geogr: Earth Environ* 27:230–259
- Ossysek S, Geist J, Werner P, Raeder U (2020) Identification of the ecological preferences of *Cyclotella comensis* in mountain lakes of the northern European Alps. *Arct Antarct Alp Res* 52:512–523
- Panizzo VN, Mackay AW, Rose NL, Rioual P, Leng MJ (2013) Recent palaeolimnological change recorded in Lake Xiaolongwan, northeast China: climatic versus anthropogenic forcing. *Quat Int* 290:322–334
- Pappas JL, Stoermer EF (1996) Quantitative method for determining a representative algal sample count. *J Phycol* 32:693–696
- Payne RJ, Egan J (2019) Using palaeoecological techniques to understand the impacts of past volcanic eruptions. *Quat Int* 499:278–289
- Potapova MG, Aycock L, Bogan D (2020) *Discostella lacuskarluki* (Manguin ex Kociolek & Reviers) comb. nov.: a common nanoplanktonic diatom of Arctic and boreal lakes. *Diatom Res* 35:55–62
- Rapp A (1984) Nivation hollows and glacial cirques in Söderåsen, Scania, South Sweden. *Geogr Ann Ser A Phys Geogr* 66:11–28
- Reavie ED, Sgro GV, Estep LR, Bramburger AJ, Shaw Chraïbi VL, Pillsbury RW, Cai M, Stow CA, Dove A (2017) Climate warming and changes in *Cyclotella sensu lato* in the Laurentian Great Lakes. *Limnol Oceanogr* 62(2):768–783
- Renberg I (1990) A procedure for preparing large sets of diatom slides from sediment cores. *J Paleolimnol* 4:87–90
- Renberg I, Hansson H (2010) Freeze corer No. 3 for lake sediments. *J Paleolimnol* 44:731–736
- Renberg I, Korsman T, Birks HJ (1993) Prehistoric increases in the pH of acid-sensitive Swedish lakes caused by land-use changes. *Nature* 362(6423):824–827
- Rey F, Gobet E, van Leeuwen JF, Gilli A, van Raden UJ, Hafner A, Wey O, Rhiner J, Schmocker D, Zünd J, Tinner W (2017) Vegetational and agricultural dynamics at Burgäschisee (Swiss Plateau) recorded for 18,700 years by multi-proxy evidence from partly varved sediments. *Veg Hist Archaeobotany* 26:571–586
- Ringberg B (1984) Cyclic Lamination in proximal varves reflecting the length of summers during late Weichsel in southernmost Sweden. In: Möner N-A, Karlén W (eds) Climatic changes on a yearly to millennial basis: geological, historical and instrumental records. Springer, Netherlands, Dordrecht, pp 57–62
- Rosén P, Hammarlund D (2007) Effects of climate, fire and vegetation development on Holocene changes in total organic carbon concentration in three boreal forest lakes in northern Sweden. *Biogeosciences* 4(6):975–984
- Rosén P, Hall R, Korsman T, Renberg I (2000) Diatom transfer-functions for quantifying past air temperature, pH and total organic carbon concentration from lakes in northern Sweden. *J Paleolimnol* 24:109–123
- Rühland KM, Smol JP, Pienitz R (2003) Ecology and spatial distributions of surface-sediment diatoms from 77 lakes in the subarctic Canadian treeline region. *Can J Bot* 81:57–73
- Rühland K, Paterson AM, Smol JP (2008) Hemispheric-scale patterns of climate-related shifts in planktonic diatoms from North American and European lakes. *Glob Chang Biol* 14:2740–2754
- Saros JE, Anderson NJ (2015) The ecology of the planktonic diatom *Cyclotella* and its implications for global environmental change studies. *Biol Rev Camb Philos Soc* 90:522–541
- Saros JE, Michel TJ, Interlandi SJ, Wolfe AP (2005) Resource requirements of *Asterionella formosa* and *Fragilaria crotonensis* in oligotrophic alpine lakes: implications for recent phytoplankton community reorganizations. *Can J Fish Aquat Sci* 62:1681–1689
- Saros JE, Strock KE, Mccue J, Hogan E, Anderson NJ (2014) Response of *Cyclotella* species to nutrients and incubation depth in Arctic lakes. *J Plankton Res* 36(2):450–460
- Sivarajah B, Rühland KM, Labaj AL, Paterson AM, Smol JP (2016) Why is the relative abundance of *Asterionella*

- formosa* increasing in a Boreal Shield lake as nutrient levels decline? J Paleolimnol 55:357–367
- SLU (2024) Swedish University of Agricultural Sciences (SLU). Data hosting lakes and streams, and data hosting agriculture land. Station ID: 00198165. <https://miljodata.slu.se/mvm>. Accessed 15 Jan 2024
- Šmilauer P, Lepš J (2014) Multivariate analysis of ecological data using CANOCO 5. Cambridge University Press
- Smol JP (1985) The ratio of diatom frustules to chrysophycean statospores: a useful paleolimnological index. Hydrobiologia 123:199–208
- Stone J, Fritz SC (2004) Three-dimensional modeling of lacustrine diatom habitat areas: improving paleolimnological interpretation of planktic: benthic ratios. Limnol Oceanogr 49:1540–1548
- Stone JR, Saros JE, Pederson GT (2016) Coherent late-Holocene climate-driven shifts in the structure of three rocky mountain lakes. Holocene 26:1103–1111
- Sverdrup H, Martinson L, Alveteg M, Moldan F, Kronnäs V, Munthe J (2005) Modeling recovery of Swedish ecosystems from acidification. AMBIO J Human Environ 34(1):25–31
- Szczerba A, Monika R, Tylmann W (2023) Modern diatom assemblages and their association with meteorological conditions in two lakes in northeastern Poland. Ecol Ind 147(110028):110028
- Thordarson T, Self S (2003) Atmospheric and environmental effects of the 1783–1784 Laki eruption: a review and reassessment. J Geophys Res. <https://doi.org/10.1029/2001JD002042>
- Wang L, Rioual P, Panizzo VN, Lu H, Gu Z, Chu G, Yang D, Han J, Liu J, Mackay AW (2012) A 1000-yr record of environmental change in NE China indicated by diatom assemblages from maar lake Erlongwan. Quat Res 78(1):24–34
- Williams DM (2019) Spines and homologues in “araphid” diatoms. Plant Ecol Evol 152(2):150–162
- Wunsam S, Schmidt R, Müller J (1999) Holocene lake development of two Dalmatian lagoons (Malo and Veliko Jezero, Isle of Mljet) in respect to changes in Adriatic sea level and climate. Palaeogeogr Palaeoclimatol Palaeoecol 146:251–281
- Zillén L (2003) Setting the Holocene clock using varved lake sediments in Sweden, LUNDQUA Thesis 50. Department of Geology, GeoBiosphere Science Centre, Lund University, Quaternary Sciences
- Zolitschka B, Francus P, Ojala AEK, Schimmelmann A (2015) Varves in lake sediments—a review. Quat Sci Rev 117:1–41

Publisher's Note Springer Nature remains neutral with regard to jurisdictional claims in published maps and institutional affiliations.